Experimental section

1. Materials

All materials were purchased from Sigma-Aldrich unless specified otherwise. PCBA powders (99%) were purchased from Solenne BV. The CH_3NH_3I (MAI) was synthesized as previously reported.[1] 55.7 ml of CH_3NH_2 (40% in methanol, Junsei Chemical Co.) was reacted with 60 ml of HI (48% in H_2O) in a glass beaker at 0 ºC for 2 hours. The precipitate was recovered by evaporation at 60 ºC for 2 hours. Precipitated MAI was then rinsed in diethyl ether 3 times and dried at 60 ºC in a vacuum oven for 12 hours.

2. Interfacial modifications

A Si prism (40 × 10 × 0.4 mm^3, 45° bevels) was used as the substrate for MIR-IRAS measurement. The substrates for XPS and solar cells were ITO coated glasses.

A TiO_2 layer with a thickness of 50 nm was sputtered onto substrates. Subsequently the TiO_2 layer was annealed at 450 °C for 1 hour and 500 °C for 30 minutes in the ambient air. Before the surface modification, the TiO_2-coated substrates were further treated in a UV-Ozone cleaner for 15 minutes.

The PCBA-modification was performed as we previously reported.[2] The substrates were dipped in a 0.2 mg/mL PCBA solution in dichlorobenzene (DCB) for 1 hour, and then rinsed and ultrasonically cleaned in DCB to remove physically adsorbed PCBA molecules. DMF-modification was performed by dropping 40 μL of DMF on the TiO_2 surface. After 1 minute, the excessive DMF was spun off the substrate at 3000 rpm.

3. Fabrication of perovskite solar cells

In order to rule out the effect of leakage current due to direct contact of Spiro-MeOTAD and TiO_2 layer on the electrical properties of the perovskite solar cells, the vapor-assisted solution process (VASP) was used to deposit pin-hole free perovskite layers on bare and

modified TiO_2 surfaces.[3] Firstly, PbI_2 layers were deposited on TiO_2 surface by thermally evaporating PbI_2 in vacuum ($<10^{-5}$ Pa) at a rate of 0.5 Å/s. The PbI_2-coated substrates were subsequently transferred into N_2-filled glovebox and placed on a hotplate. MAI powders were spread around the samples. The sample and the MAI powder were covered with a petri dish and then heated to 150 °C for 2 hours to form perovskite layers. Before depositing the hole-transporting layer, the perovskite layer were annealed at 150 °C in N_2 atmosphere for 10 minutes. The solution of the hole transporting material was prepared by dissolving 90 mg Sprio-MeOTAD in 1 mL chlorobenzene. 50 μL lithium bis(trifluoromethylsulphonyl)-imide (170 mg/mL in acetonitrile) and 20 μL 4-tert-butylpyridine were then added into the solution. The hole transporting layer was deposited on perovskite layer by spin-coating at 2500 rpm for 60 seconds. Finally, a gold layer with a thickness of 80 nm was thermally evaporated to form the cathode. All devices were left in a desiccator for 12 hours before measurements.

4. Characterization

MIR-IRAS measurement setup is similar as that we used to study the perovskite bulk.[4] An ultrathin layer (less than 20 nm) of $CH_3NH_3PbI_3$ perovskite was spin-coated from a precursor solution (0.05 M MAI and 0.05 M PbI_2 in DMF) on bare and PCBA-modified TiO_2 surfaces. The perovskite layers were then annealed at 100 °C for 5 minutes to remove solvent molecule in the bulk. In order to prevent the reaction of perovskite and surface modifiers with the ambient air, all depositions and measurements were carried out in a nitrogen-filled glove box.

The core-levels of the elements near the surface was evaluated by XPS (AXIS Nova, Kratos Analytical) with a monochromatized X-ray of Al Kα line at 1487 eV and a take-off angle for photoelectron of 90° (perpendicular to the surface).

The current density-voltage (J-V) curves of perovskite solar cells were characterized in the dark and under simulated AM 1.5 illumination (100 mW/cm^2).

5. *Ab-initio* simulation

Vibrational frequencies and intensities were calculated by Gaussian 09 in which the Becke, 3-parameter, Lee-Yang-Parr functional (B3LYP)[5-7] with 6-31G(d',p') basis set[8] was used. We used the scaling factor as 0.9613 in the calculations of vibrational frequencies[9,10].

Additional figures

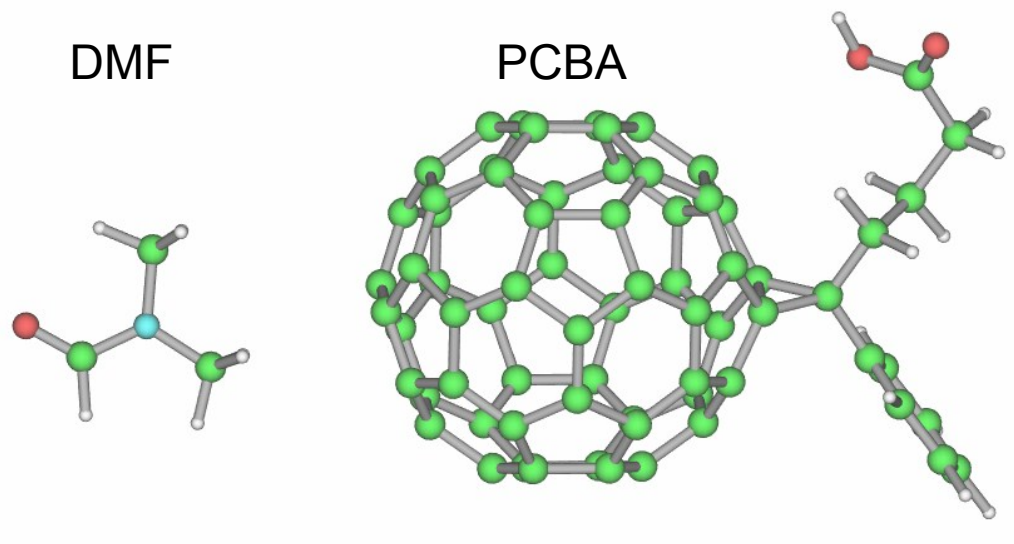

Fig. S1 The DMF and PCBA molecular structure optimized using Gaussian 09 in which the Becke, 3-parameter, Lee – Yang – Parr functional (B3LYP) with 6-31G(d',p') basis set was used.

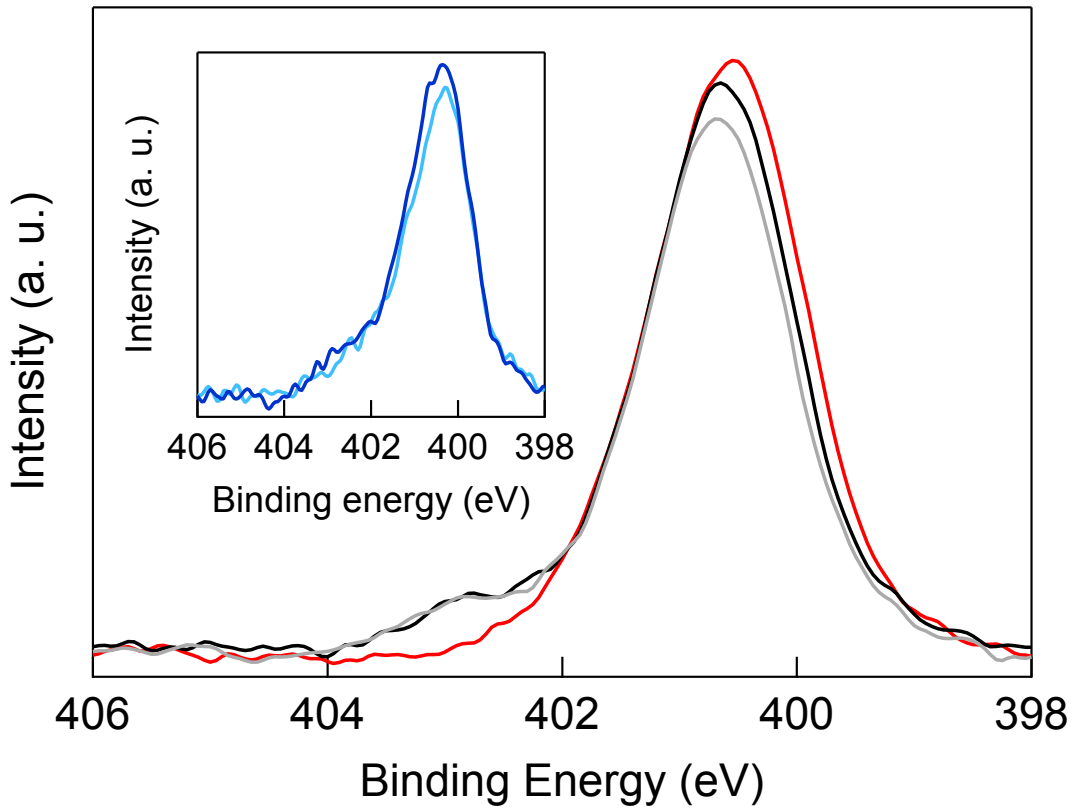

Fig. S2 XPS N1s spectra of bare TiO_2 surface (red), DMF on TiO_2 before (black) and after (gray) annealing at 150 °C for 30 minutes. The inset displays the enlarged spectra of PCBA-modified TiO_2 surfaces without (dark blue) and with (light blue) DMF treatment.

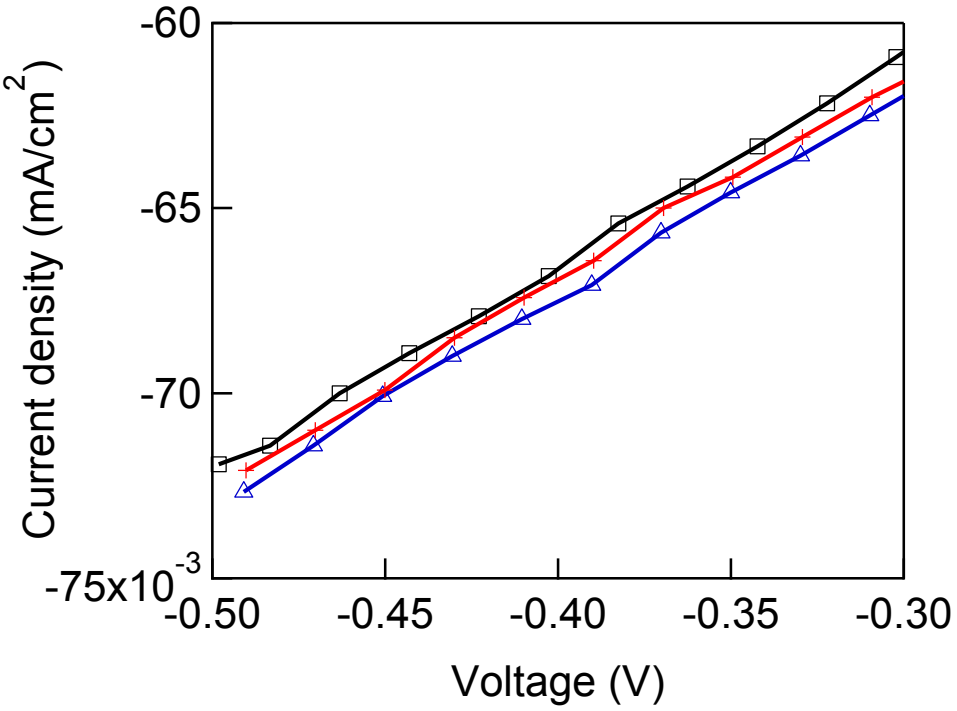

Fig. S3 The enlarge figure of the dark J-V curve in the region of −0.5~ −0.3 V.

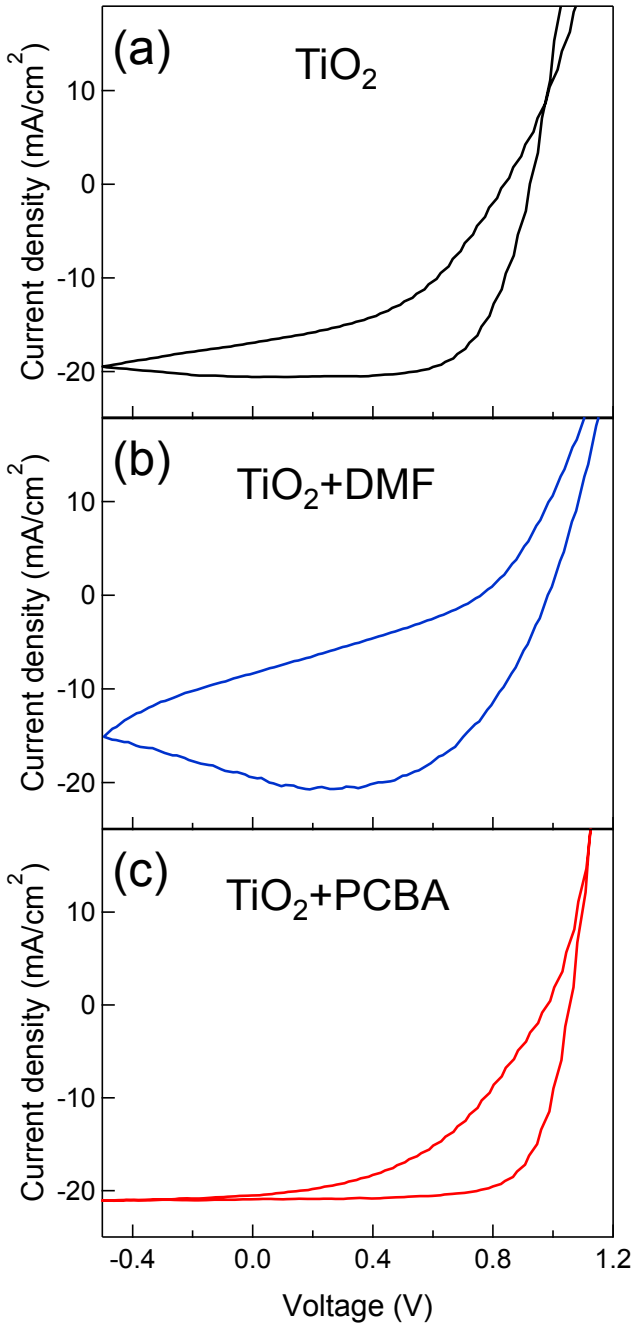

Fig. S4 Hysteresis behaviors of solar cells fabricated on the bare, DMF-adsorbed and PCBA-modified TiO_2 surfaces (scan rate = 0.1 V/s).

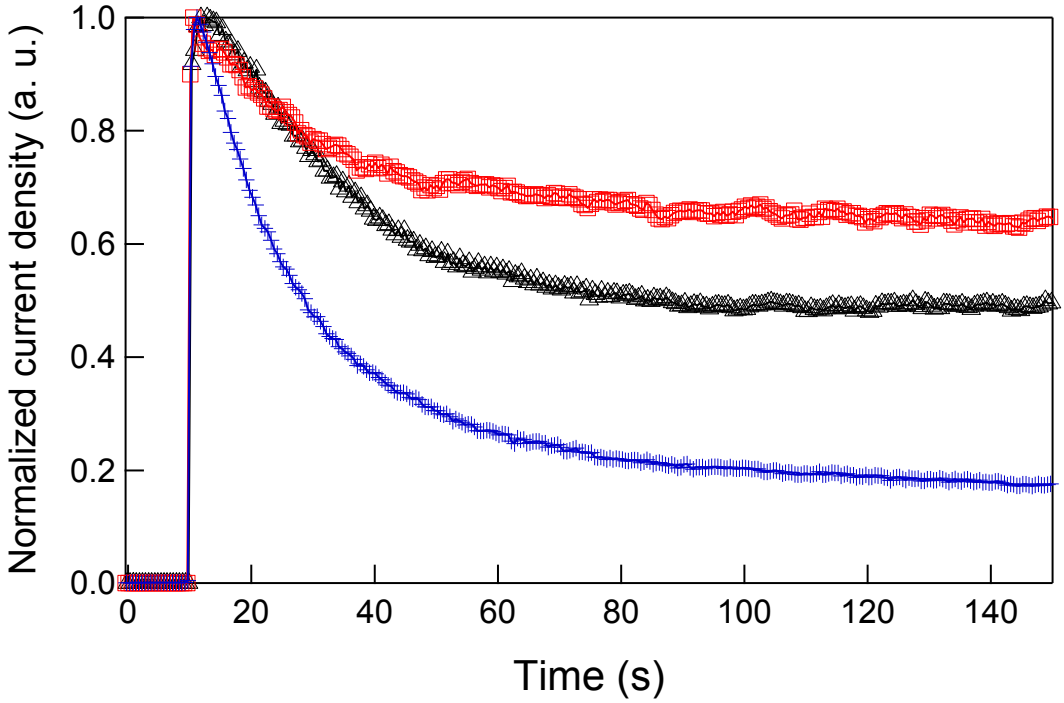

Fig. S5 Stabilized power-output tracking of the solar cells fabricated on the bare (black triangle), DMF-adsorbed (blue cross) and PCBA-modified TiO_2 (red square) surfaces. The devices were all biased at 0.7V for comparison.

Discussion about the error in resistance approximation

1. Error of shunt resistance

The current density J and voltage V of a solar cell can be generally characterized using a single diode model.[11] The relation between J and V is given by:

$$J = J_{ph} - J_0\left[exp\left(\frac{q(V + R_sJ)}{nk_BT}\right) - 1\right] - \frac{V + R_sJ}{R_{sh}}$$

In the dark condition, we have $J_{ph} = 0$. If we set V'=V+R_sJ, then we have:

$$J = -J_0\left[exp\left(\frac{qV'}{nk_BT}\right) - 1\right] - \frac{V'}{R_{sh}}$$

In the shown region in Fig. S3, since the current is very small and the R_s of perovskite solar cells is normally much smaller than 100 Ω,[12-14] V' should be very close to V.

So -dJ/dV is approximated by:

$$-\frac{dJ}{dV} \approx \frac{qI_0}{nk_BT}exp\left(\frac{qV}{nk_BT}\right) + \frac{1}{R_{sh}}$$

I_0 should be close to J_{sc} when $R_{sh} \gg R_s$.[5] Also, the ideal factor n is typically in the range of 1<n<2 in a well-behaved solar cell.[14] The value of the first part of the above equation should be less than $1.6 \times 10^{-6}\ \Omega^{-1}cm^{-1}$ when V=–0.4 V. Even we use the largest value to calculate the error when estimating the R_{sh} from the slope of the J-V curve, the error is just 3%.

2. Error of series resistance

From the relation between J and V in a single diode model, -dV/dJ is approximated by:[5]

$$-\frac{dV}{dJ} = \frac{\frac{nk_BT}{q}}{J_{sc} - J - \frac{V - R_s(J_{sc} - J) - \frac{nk_BT}{q}}{R_{sh}}} + R_s$$

We extract the R_s value from the region where the current density close to –40 mA/cm^2. And due to the large value of R_{sh}, the above equation can be reduced to:

$$-\frac{dV}{dJ} = -\frac{nk_BT}{qJ} + R_s$$

Because the value of n is in the region of 1<n<2, the error when estimate the R_s from the slope of the J-V curve should be around 0.65 to 1.3 Ω·cm^2.

Reference

1. J. H. Heo, S. H. Im, J. H. Noh, T. N. Mandal, C.-S. Lim, J. A. Chang, Y. H. Lee, H. Kim, A. Sarkar, M. K. Nazeeruddin, M. Grätzel and S. I. Seok, Efficient inorganic–organic hybrid heterojunction solar cells containing perovskite compound and polymeric hole conductors, *Nat. Photonics*, 2013, **7**, 486–491.
2. T. Ma, J. Zhang, R. Kojima, D. Tadaki, Y. Kimura and M. Niwano, Investigation of TiO_2 Surface Modification with [6,6]-Phenyl-C_{61}-butyric Acid for Titania/Polymer Hybrid Solar Cells, *Jpn. J. Appl. Phys.*, 2013, **52**, 112301.
3. Q. Chen, H. Zhou, Z. Hong, S. Luo, H.-S. Duan, H.-H. Wang, Y. Liu, G. Li and Y. Yang, Planar Heterojunction Perovskite Solar Cells via Vapor-Assisted Solution Process, *J. Am. Chem. Soc.*, 2014, **136**(2), 622–625.
4. T. Ma, M. Cagnoni, D. Tadaki, A. Hirano-Iwata and M. Niwano, Annealing-induced chemical and structural changes in tri-iodide and mixed-halide organometal perovskite layers, *J. Mater. Chem. A*, 2015, **3**, 14195–14201.
5. A. D. Becke, *J. Chem. Phys.*, 1993, **98**(2), 1372.
6. K. Kim and K. D. Jordan, *J. Phys. Chem.*, 1994, **98**(40), 10089.
7. P. J. Stephens, F. J. Devlin, C. F. Chabalowski and M. J. Frisch, *J. Phys. Chem.*, 1994,

98(45), 11623.

8. J. A. Pople, *Proceedings of the Summer Research Conference on Theoretical Chemistry, Energy Structure and Reactivity,* New York, USA (1973).
9. Chr. Plutzer, E. Nir, M. S. de Vries and K. Kleinermanns, *Phys. Chem. Chem. Phys.*, 2001, **3**, 5466.
10. X. Zhang, Y. Zhan, D. Chen, F. Wang, L. Wang, *Dyes and Pigments*, 2012, **93**, 1408.
11. K.-i. Ishibashi, Y. Kimura and M. Niwano, An extensively valid and stable method for derivation of all parameters of a solar cell from a single current-voltage characteristic, *J. Appl. Phys.*, 2008, **103**, 094507.
12. Y. Wu, X. Yang, H. Chen, K. Zhang, C. Qin, J. Liu, W. Peng, A. Islam, E. Bi, F. Ye, M. Yin, P. Zhang and L. Han, Highly compact TiO_2 layer for efficient hole-blocking in perovskite solar cells, *Appl. Phys. Express*, 2014, **7**, 052301.
13. E. J. Juarez-Perez, M. Wuβler, F. Fabregat-Santiago, K. Lakus-Wollny, E. Mankel, T. Mayer, W. Jaegermann and I. Mora-Sero, Role of the Selective Contacts in the Performance of Lead Halide Perovskite Solar Cells, *J. Phys. Chem. Lett.*, 2014, **5**, 680−685.
14. J. Shi, J. Dong, S. Lv, Y. Xu, L. Zhu, J. Xiao, X. Xu, H. Wu, D. Li, Y. Luo and Q. Meng, Hole-conductor-free perovskite organic lead iodide heterojunction thin-film solar cells: High efficiency and junction property, *Appl. Phys. Lett.*, 2014, **104**, 063901.